

Design of a Fully Reconfigurable Multifunctional Non-Reciprocal Quise Reflection-Less Interdigital BPF

Yasir M. Alabedi¹, Seyed Vahab AL-Din Makki¹

Department of Electrical Engineering, Faculty of engineering
 Razi University, Kermanshah, Iran
 yasir.alabedi@atu.edu.iq, v.makki@razi.ac.ir

Nasr Alkhafaji²

Department of Communication Engineering Techniques, Engineering Technical College of Al-Najaf, Al-Furat Al-Awsat
 Technical University, Najaf, Iraq.
 nasmomas@atu.edu.iq

Abstract— This paper presents the design, simulation, and measurement of a multifunctional nonreciprocal quasi-reflectionless bandpass filter. Initially, we designed a conventional 5-pole interdigital bandpass filter (BPF). Subsequently, a suitable absorptive component is attached to the conventional interdigital BPF in order to absorb any reflected signals, resulting in the formation of a quasi-reflectionless BPF. One can turn a normal bandpass filter (BPF) into a nonreciprocal BPF by employing the Spatial Temporal Modulation (STM). In order to obtain a multifunctional bandpass filter, all of these features must be combined into a single filter. Therefore, pin diodes can operate as switches to control the response of multifunctional bandpass filters. The proposed filter can provide multiple response states, including reflective bandpass filters, quasi-reflectionless bandpass filters (with one port and two ports), non-reciprocal bandpass filters, and non-reciprocal quasi-reflectionless bandpass filters. The filter was designed using a Fr4 substrate and a CNC machine. The measured results demonstrate a high level of agreement with the simulated results.

Keywords- multi-functional filter; reflectionless; non-reciprocal; BPF; adjustable filter; reconfigurable filter

1. INTRODUCTION

Wireless communication technology has become an essential and integral aspect of our modern lives. Therefore, it is important to continuously enhance the primary elements of the RF front-end chain. The filter is an RF component that is responsible for selecting the operating bandwidth with as little noise as possible [1]. In conventional filters, the signals passing within the desired frequency range are transmitted to the output terminals, while the signals falling beyond this range are reflected back to the source [2]. Consequently, a new classification of filters, referred to as reflectionless filters or absorptive filters, has been developed. These filters efficiently dissipate the reflected signals inside lossy components, rather than reflecting them back to the input port [3]. The reflectionless filter structure is depicted in Figure (1) as a conceptual circuit diagram.

Additionally, non-reciprocal devices, such as isolators and circulators, play a crucial role in the construction of communication systems. These devices are used to protect active components from signals reflecting back and/or eliminate the interference between the receive and transmit channels for full duplex communication [4,5, 6]. Traditionally, non-reciprocal devices are implemented using ferromagnetic materials, which are known to be bulky and difficult to combine with other circuits [7, 8, 9, 10]. [11]. Several research teams have reported the development of magnet-less nonreciprocal bandpass filters (BPFs) that utilize time-modulated resonators to enable unidirectional signal propagation ($|S_{21}| \neq |S_{12}|$) [12–18]. This study presents the design of a fully reconfigurable multipurpose bandpass filter (BPF) to enhance the functionality and reduce the size of the RF front-end.

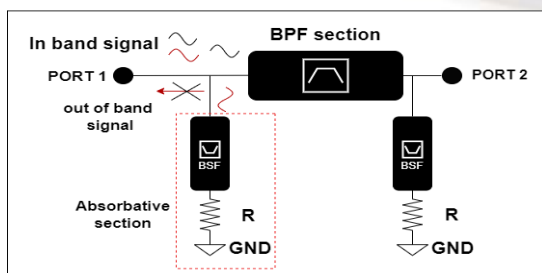
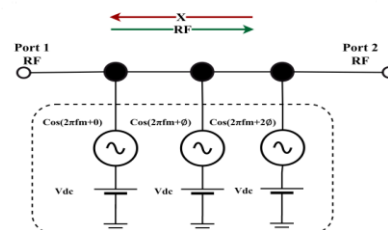


Figure 1. Structure of the proposed quasi-Reflectionless bandpass filter



(a)

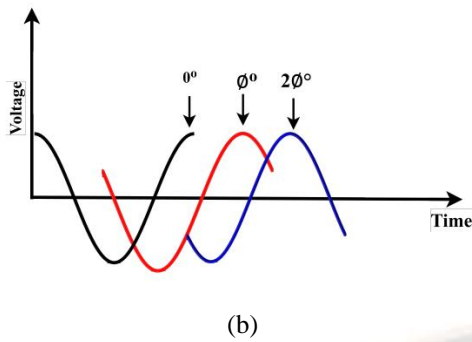


Figure 2: (a) Concept of magneticless non-reciprocal BPF based on modulated RF resonators digram (b) Resonators Phase shifting

The non-reciprocity is attained by employing the STM technique on the resonators of the bandpass filters (BPF) with progressively phase-shifted AC signals. On the other hand, the QR BPF can be achieved by utilizing suitable absorptive materials.

2 .METHODOLOGY

This section aims to provide an obvious way to explain the steps that will be followed to come up with the final design proposed in this paper, as shown in Figure 3. The first step is how to design a 5-pole band pass filter (BPF). At this point, the filter is the conventional reflective filter type. To achieve a reflectionless filter type, we design absorptive stubs. The objective is to optimize the impedance characteristics of the absorptive part to achieve a wider range of impedance matching in and out of the band of the interested frequency. Next, the lossy (i.e., absorptive) stubs integrate both reflective filter types. A quasi-reflective response was achieved by connecting absorptive and conventional interdigital BPF. In the next step, a non-reciprocal BPF was designed using the spatial-temporal modulation (STM) technique. After that, a multifunctional non-reciprocal QR BPF will be designed using control switches (pin diodes).

2.1 A CONVENTIONAL 5-POLE INTERDIGITAL BPF

In this subsection, a 5-pole interdigital BPF is designed and analyzed. For this design, the fractional bandwidth FBW = 0.52 at a resonant frequency $f_0 = 1.8$ GHz, $n = 5$ (Chebyshev ripple of 0.1dB). The LPF prototype parameters, with respect to a normalised lowpass cutoff frequency $\omega_c = 1$, are $g_0 = g_6 = 1$, $g_1 = g_5 = 1.1468$, $g_4 = g_2 = 1.3712$, and $g_3 = 1.9750$. To accomplish coupling fields fringe across neighboring resonators with a separation of $s_i, i+1$ for $i = 1 - n-1$:

$$m_{i,j+1} = \frac{FBW}{\sqrt{g_i g_{j+1}}} \quad (1)$$

$$\text{Where } FBW = \frac{f_2 - f_1}{f_0}, f_0 = \sqrt{f_1 f_2}$$

Where, g_i and g_{i+1} represents the element values of a ladder-type lowpass prototype filter with a normalized cutoff frequency at $\Omega_c = 1$, f_1 and f_2 are the upper and lower resonant frequencies 1.1, 2.1 GHz respectively, f_0 is center frequency (1.8 GHz). The mutual coupling matrix (M) can be calculated from (1). The filter's actual dimensions ($w_1, w_2, \dots, w_5, s_{0,1}, s_{1,2}, s_{2,3}, s_{3,4}, s_{4,5}$) may

be determined [19]. the parameter design of 5-pole interdigital BPF listed in table (1).

$$M = \begin{bmatrix} 0 & 0.7 & 0 & 0 & 0 & 0 & 0 \\ 0.7 & 0 & 0.4138 & 0 & 0 & 0 & 0 \\ 0 & 0.4138 & 0 & 0.3153 & 0 & 0 & 0 \\ 0 & 0 & 0.3153 & 0 & 0.3153 & 0 & 0 \\ 0 & 0 & 0 & 0.3153 & 0 & 0.4138 & 0 \\ 0 & 0 & 0 & 0 & 0.4138 & 0 & 0.7 \\ 0 & 0 & 0 & 0 & 0 & 0.7 & 0 \end{bmatrix}$$

Table 1 5-pole interdigital BPF parameters (mm)

Lt	R.via	Wf	L1=L5	L3	Lf
13	0.2	1.85	29.9	25.54	11.5
W	S1,2=S4,5	S2,3=S3,4	L2=L4		
2.39	0.2	0.4	25.54		

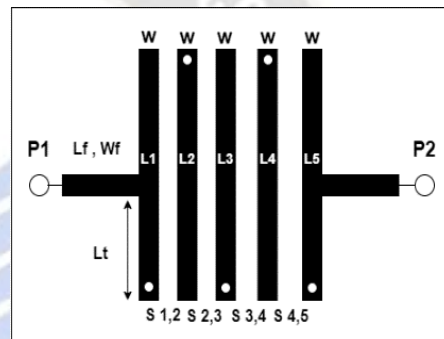


Figure 3 : Conventional 5-pole BPF structure.

2.2 QUASI REFLECTIONLESS INTERDIGITAL BPF DESIGN

This part will outline the process of designing a QR interdigital bandpass filter (BPF) in two distinct steps. The initial stage involves the design of the absorptive component. Stubs can be utilised to create absorptives in a T-shape configuration. A lumped resistor is attached to the end of a band-stop filter (BSF) to absorb undesirable signals, as depicted in figure 4. The resistor has the capability to absorb undesired power. The absorptive input impedance (Z_{in-ab}) can be determined by applying the following formulas:

$$Z_{in-ab} = \frac{Z_1 + j Z_A \tan(\theta)}{Z_A + j Z_1 \tan(\theta)} \quad (2)$$

$$\text{Where } Z_2 = \frac{R + j Z_A \tan(\theta)}{Z_A + j R \tan(\theta)}, Z_3 = -j Z_B \cot(\theta)$$

$$Z_1 = Z_2 // Z_3, Z_1 = \frac{Z_2 Z_3}{Z_2 + Z_3}$$

The next step in designing QR interdigital BPF is connecting the absorptive for each port of BPF. By connecting these absorptives to each port, it is possible to prevent the reflection of undesired signals back to the input port. Figure 5 demonstrates the conversion of a conventional bandpass filter into a quasi-reflectionless bandpass filter. Due to the symmetric design, both S_{11} and S_{22} will exhibit identical characteristics. Additionally, the suggested filter will effectively suppress reflected signals. The input impedance of a two-port quadrature resonator interdigital bandpass filter (Z_{in-QR2}) can be derived using the following equation:

$$Z_{in-QR2} = Z_{in-ab1} // Z_{in-BPF} // Z_{in-ab2} \quad (3)$$

where (Z_{in-ab}) is the input impedance of absorptive that was calculated in eq. (2). parameter design of 5-pole QR interdigital BPF listed in table (2).

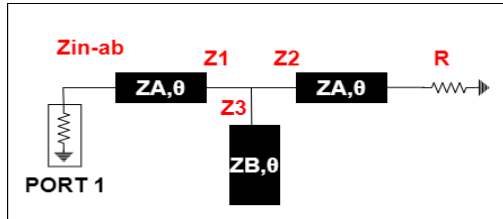


Figure. 4 General configuration of absorptive.

Table 2. parameters that used for designing a QR 5-pole interdigital BPF

Lt	Lf1	Wf1	Lf2	Wf2
11.059	10.383	3.4	12.425	1.85
L1=L5		L2=L4		L3
22.75		19.02		18.43
S1,2=S4,5		S2,3=S3,4		R
0.2		0.36		100
LAB1		WAB1	WAB2	LAB2
18.825		1.85	1.15	40.25
LAB3		WAB3	W	
20.05		0.65	2.39	

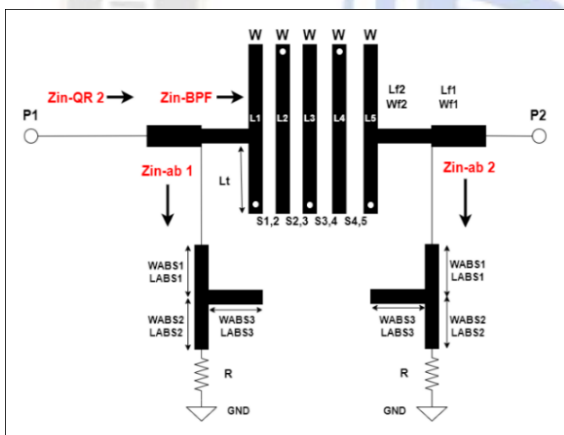


Figure 5. layout of 5-pole two port QR interdigital BPF

2.3 NONRECIPROCAL INTERDIGITAL BANDPASS FILTER DESIGN

This subsection designs a nonreciprocal interdigital BPF. Fig. 6 shows the conceptual circuit topology of the proposed 5-pole non-reciprocal filter. To achieve a magnet-less non-reciprocal BPF ($|S_{21}| \neq |S_{12}|$) based on STM, the resonators (R1, R2, R3, R4, and R5) are modulated in time and space by modulating the capacitors as follows:

$$C_i(t) = C_0 + \Delta C \sin [2\pi f_m t + (i)\varphi]; \quad (i = 1: 5) \quad (4)$$

where ΔC is the amplitude of the capacitance variation, f_m is the modulation frequency, and φ is the phase difference between the two modulation sources. Here, we define:

$$D_m = \Delta C / C_0 \quad (5)$$

D_m is the modulation index. The center frequency f_0 of the non-reciprocal filter is determined by the static inductance L_0 and static capacitance C_0 . When there is no modulation, i.e., $D_m = 0$, the circuit in figure (6) is essentially a conventional 5-pole filter. When the capacitors are sinusoidally modulated as in (4), intermodulation (IM) products at $f_{RF} \pm k f_m$ ($k = 1; 2; 3, \dots$) will be generated in the circuit. It can be shown that power conversion between f_{RF} and these IM frequencies is non-reciprocal.

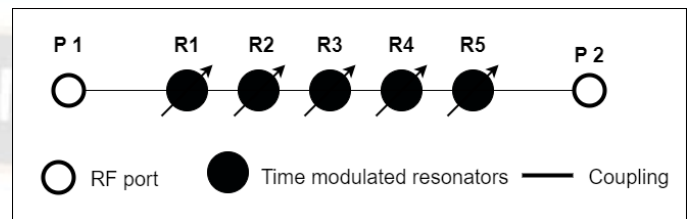


Figure (6): None reciprocal BPF using 5 modulated resonators. When the modulation parameters are set correctly, the power at the intermodulation (IM) frequencies can be collected at the radio frequency (fRF), and there will be low loss of signal in one direction. However, in the other direction, the signal power spreads from fRF to the IM frequencies, leading to significant attenuation. [20].

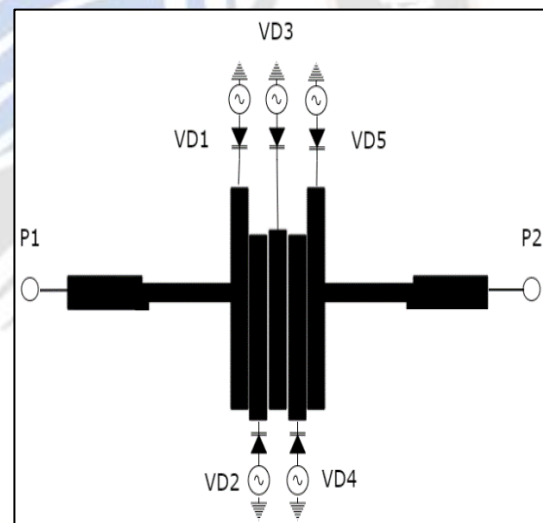


Figure (6) nonreciprocal interdigital BPF structure

3. MULTIFUNCTIONAL NON RECIPROCAL AND QR BPF

This chapter presents the design of a multifunctional bandpass filter (BPF) by combining the methodologies discussed in the preceding chapter into a single filter. The filter response can be controlled by turning on or off the switches located at specified positions, as illustrated in Figure (7). Switches Sw1 and Sw2 can be utilized to convert a reflective bandpass filter (BPF) into a reflectionless BPF, and vice versa. Additionally, by activating one switch and deactivating the other, or by activating both switches, it is possible to transform a single-port QR BPF into a two-port QR BPF.

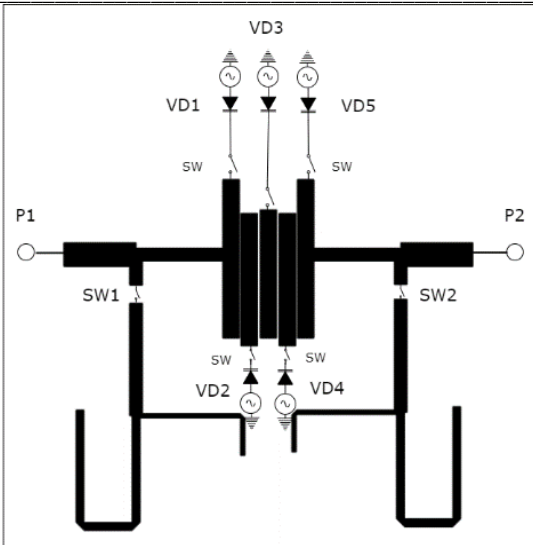


Figure (7) nonreciprocal QR interdigital BPF structure

4. RESULTS OF THE PROPOSED MULTIFUNCTIONAL BPF

In this section, the results of all previous designs will be detailed. The initial design of the 5-pole interdigital bandpass filter (BPF) in subsection 2.1 is centred at a frequency of 1.8 GHz. This frequency is achieved when all the switches (pin diodes) in the multifunctional BPF structure, as shown in figure (7), are in the off state. Currently, the proposed structure will produce a bandpass filter (BPF) response, as depicted in figure (8).

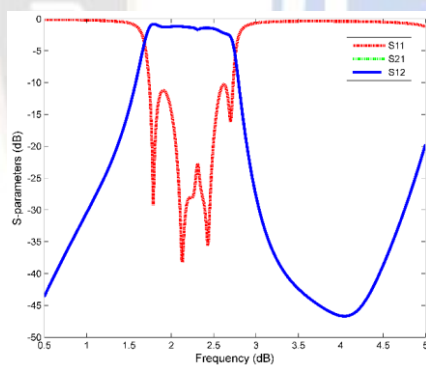


Figure (8): S-parameters of the proposed filter at BPF state

To obtain a single port QR-BPF, the next step is to activate Sw1 and turn off all other switches. Refer to figure (9) where $|S11|$ is not equal to $|S22|$. The value of $|S22|$ is zero for all frequencies outside the desired range, while it is less than 10 dB within the desired range. The signal attenuation at both the in-band and out-of-band frequencies is below 10 dB. Activating both switches (Sw1 and Sw2) will result in getting of a dual-port (QR-BPF), as depicted in figure (10). The absorption ratio is high both inside and outside the desired frequency range, and the magnitudes of S11 and S22 are equal. The bandwidth (BW) is 1.215 GHz, as indicated by the S21 measurement, which spans from $f1=1.587$ GHz to $f2=2.802$ GHz. Furthermore, the S11, which has a magnitude smaller than -10dB, spans from 709.4 MHz to 3.884 GHz.

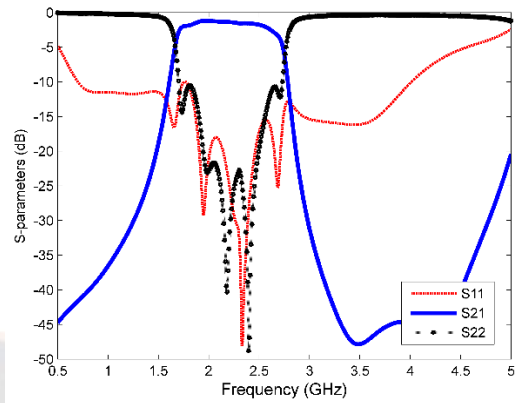


Figure (9): S-parameters of the QR one port BPF

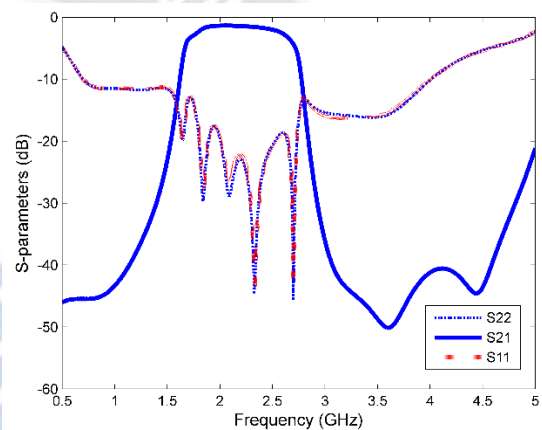


Figure (10): S-parameters of the QR two port BPF

Also, by turning on all switches expect Sw1 and Sw2 the non-reciprocal BPF response will be get, as shown in figure (11). It's clear the effect of STM is done by connecting varactor diodes for all resonators. Where $f_m = 500$ MHz, $\phi_1=0$, $\phi_2=68^\circ$, $\phi_3=74.8^\circ$, $\phi_4=88.4^\circ$, $\phi_5=112.2^\circ$, $D_m = 1.8$, $|S21|$ is not equal to $|S12|$. This indicates that the transmission is unidirectional. The insertion loss of S21 is -2 dB, while it is less than -11.2 dB for S12. Finally, by activating all switches, a nonreciprocal QR-BPF response is achieved, as depicted in figure (12). In this response, the absorption ratio for a wide band is high, indicating a reflectionless situation, and the magnitudes of S21 and S12 are not equal, indicating a nonreciprocity condition.

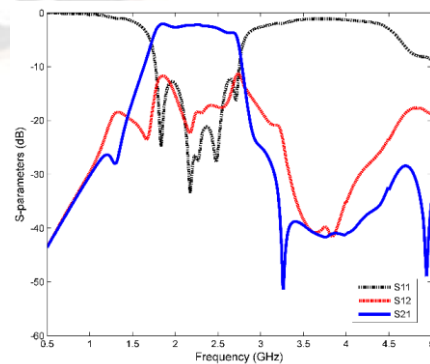


Figure (11): S-parameters of the non-reciprocal BPF

5. EXPERIMENTAL VALIDATION

To validate the proposed design 5-pole interdigital BPF and QR interdigital BPF are used in fabrication and measurement in this section. FR4 substrate with a relative dielectric constant $\epsilon_r = 4:6$, a dielectric thickness $h = 1:5$ mm, and a dielectric loss tangent $\tan(\delta D) = 0:017$ is used. The operating frequency is 1.8 GHz, and the 3 dB fractional bandwidth is 52%.

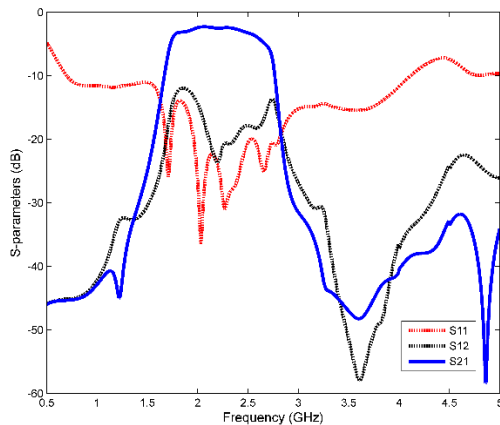


Figure (12): S-parameters of the non-reciprocal QR BPF

The first step is fabricating and measuring a 5-pole interdigital BPF. All physical dimensions of this filter are mentioned in the previous subsection (2.1) with optimize of the positions of resonators to get a better response, as shown in figure (13). Their theoretical synthesis and the software package Advanced Design System (ADS) from Keysight Technologies were used for their simulation and optimization. Their RF performances were experimentally validated with a Keysight N9917A microwave analyzer in terms of S-parameters, as shown in figures (14,15). Also, the fabrication was done using a CNC machine.

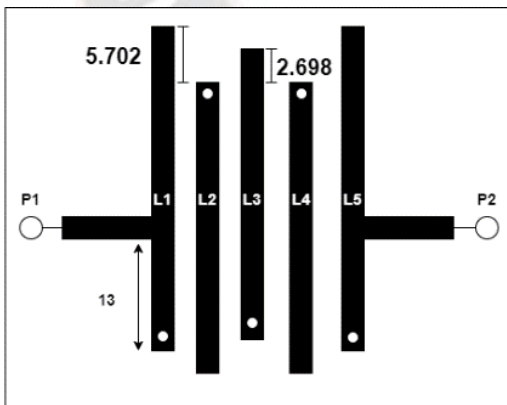


Figure 13. Structure of 5-Pole interdigital BPF

The second step of fabrication is fabricating and measuring a QR 5-pole interdigital BPF. By using the same parameters as those mentioned in subsection (2.2), we can change some positions of resonators to enhance the response of the proposed filter, as shown in figure (16). The figure (17,18) displays the measured S-parameters of a 5-Pole QR interdigital BPF. The transmission and reflection coefficients obtained from simulated

measurements are compared in Figures 19 and 20 for the Bandpass Filter (BPF) and QR BPF, respectively.

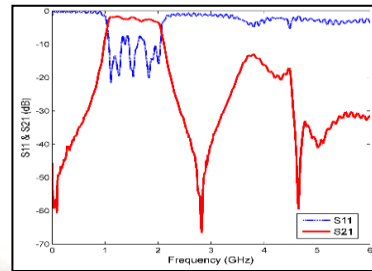


Fig. 14 Measurement result of S-parameters for 5-pole interdigital BPF (a) S21, (b) S11

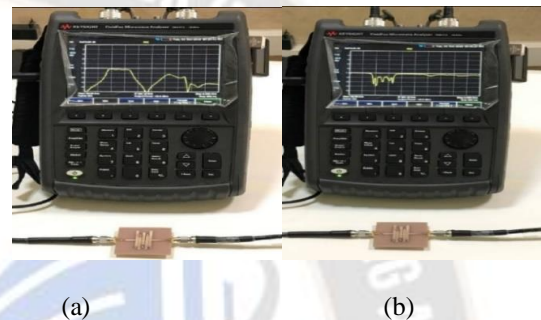


Figure 15. Measuring process of S-parameters for 5-pole interdigital BPF (a) S21, (b) S11

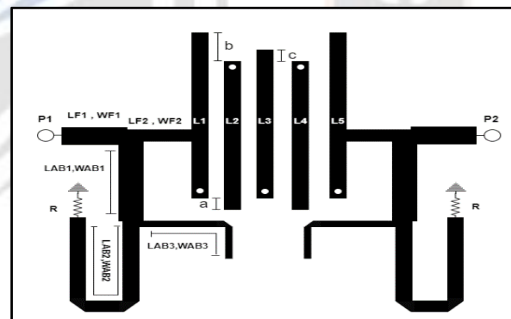


Figure. 16 (a) Structure of 5-Pole QR interdigital BPF (a=1.113, b = 4.84, c = 0.52 (mm))

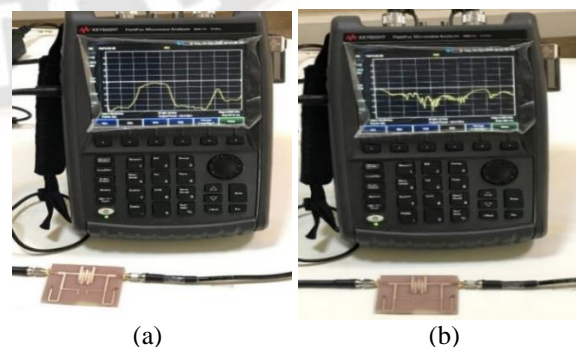


Figure 17. Measuring process of S-parameters for QR 5-pole interdigital BPF (a) S21, (b) S11

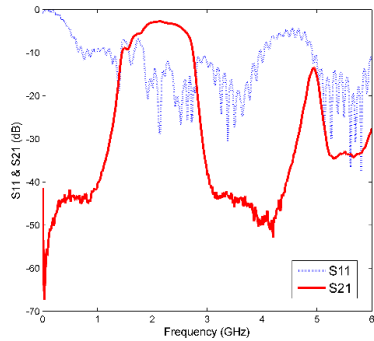


Figure. 18 Measurement result of S-parameters for QR 5-pole interdigital BPF

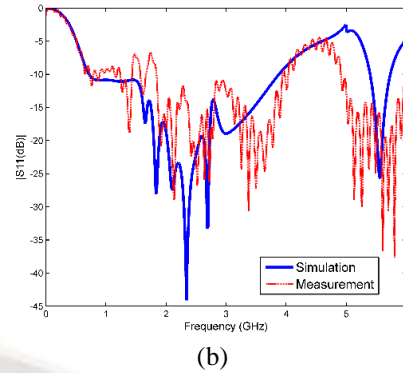


Figure 20. comparison between measurement and simulation result for response of 5-Pole QR-BPF (a)S21 and (b) S11

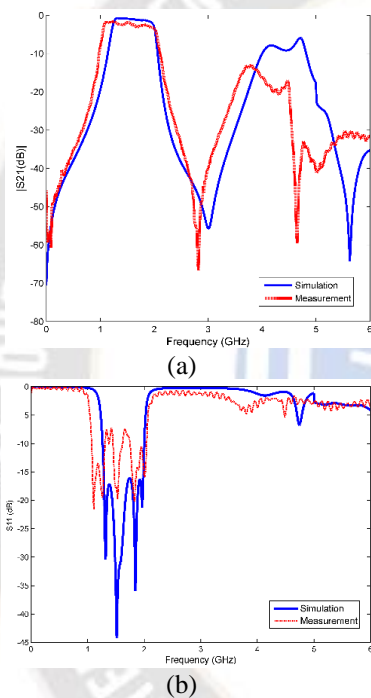
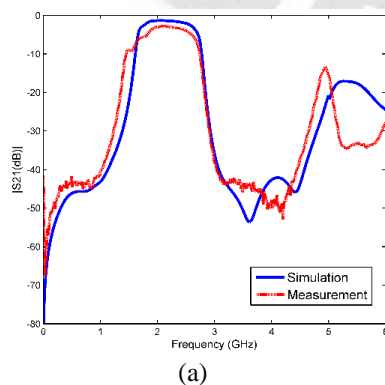


Figure 19. Comparison between measurement and simulation result for response of 5-Pole BPF (a)S21 and (b) S11.



6. CONCLUSION

The aim of this work is to create a multifunctional nonreciprocal quasi reflectionless bandpass filter that is fully configurable. This will enhance the filter's functionality and decrease the size of the RF front-end. Therefore, the suggested filter is designed using multiple phases. First, a traditional 5-pole interdigital bandpass filter (BPF) is constructed. Then, an appropriate absorptive component is coupled to the conventional interdigital BPF to create a quasi-reflectionless BPF, which is capable of absorbing reflected signals. Following that, a nonreciprocal bandpass filter (BPF) is constructed using varactor diodes to implement the Spatial Temporal Modulation (STM) approach. In addition, the filter combines all these capabilities into a single multifunctional BPF. Therefore, pin diodes can operate as switches to regulate the response of multifunctional bandpass filters. This proposed filter yields multiple response states, including reflective bandpass filters, quasi-reflectionless bandpass filters (with one port and two ports), non-reciprocal bandpass filters, and non-reciprocal quasi-reflectionless bandpass filters. The filter was constructed using Fr4 substrate and a CNC machine. The measured results demonstrate a high level of agreement with the simulated outcomes.

ACKNOWLEDGEMENT

The research work of this article is fabricated and measured in microwave lab in Department of Electrical Engineering, Razi University, Kermanshah, Iran.

FINDING

The authors of the paper reported that there is no funding associated with the work featured in the article.

CONFLICTS OF INTEREST

The authors declare no conflict of interest.

REFERENCES:

- [1] X. Wu, Y. Li, and X. Liu, "Quasi-Reflectionless Microstrip Bandpass Filters with Improved Passband Flatness and Out-of-Band Rejection," *IEEE Access*, vol. 8, pp. 160500–160514, 2020, doi: 10.1109/ACCESS.2020.3021314.
- [2] M. A. Morgan, "Think outside the band: Design and miniaturization of absorptive filters," *IEEE Microw. Mag.*, vol. 19, no. 7, pp. 54–62, 2018, doi: 10.1109/MMM.2018.2862541.

- [3] K. Da Xu, S. Lu, Y. J. Guo, and Q. Chen, "Quasi-Reflectionless Filters Using Simple Coupled Line and T-Shaped Microstrip Structures," *IEEE J. Radio Freq. Identif.*, vol. 6, pp. 54–63, 2022, doi: 10.1109/JRFID.2021.3106664.
- [4] D. M. Pozar, *Microwave Engineering*. Wiley, 2012.
- [5] Z. Yong, Z. Jian, Y. Yuanwei, C. Chen, and J. S. Xing, "A Ku-Band Novel Micromachined Bandpass Filter with Two Transmission Zeros," no. August, 2013.
- [6] J. Zhou, N. Reiskarimian, J. Diakonikolas, T. Dinc, T. Chen, G. Zussman, and H. Krishnaswamy, "Integrated full duplex radios," *IEEE Communications Magazine*, vol. 55, no. 4, pp. 142–151, April 2017.
- [7] A. Kord, D. L. Sounas, and A. Alu, "Achieving full-duplex communication: Magnetless parametric circulators for full-duplex communication systems," *IEEE Microwave Magazine*, vol. 19, no. 1, pp. 84–90, Jan 2018.
- [8] C. E. Fay and R. L. Comstock, "Operation of the ferrite junction circulator," *IEEE Transactions on Microwave Theory and Techniques*, vol. 13, no. 1, pp. 15–27, Jan 1965.
- [9] S. A. Oliver, P. Shi, N. E. McGruer, C. Vittoria, W. Hu, H. How, S. W. McKnight, and P. M. Zavracky, "Integrated self-biased hexaferrite microstrip circulators for millimeter-wavelength applications," *IEEE Transactions on Microwave Theory and Techniques*, vol. 49, no. 2, pp. 385–387, Feb 2001.
- [10] C. K. Seewald and J. R. Bray, "Ferrite-filled antisymmetrically biased rectangular waveguide isolator using magnetostatic surface wave modes," *IEEE Transactions on Microwave Theory and Techniques*, vol. 58, no. 6, pp. 1493–1501, June 2010.
- [11] X. Wu, M. Nafe, A. A. Melcón, J. Sebastián Gómez-Díaz and X. Liu, "A Non-Reciprocal Microstrip Bandpass Filter Based on Spatio-Temporal Modulation," 2019 IEEE MTT-S International Microwave Symposium (IMS), Boston, MA, USA, 2019, pp. 9-12, doi:10.1109/MWSYM.2019.8700732.
- [12] N. A. Estep, D. L. Sounas, and A. Alù, "Magnetless microwave circulators based on spatiotemporally modulated rings of coupled resonators," *IEEE Trans. Microw. Theory Techn.*, vol. 64, no. 2, pp. 502–518, Feb. 2016, doi: 10.1109/TMTT.2015.2511737.
- [13] A. Kord, D. L. Sounas, Z. Xiao, and A. Alu, "Broadband cyclical symmetric magnetless circulators and theoretical bounds on their bandwidth," *IEEE Trans. Microw. Theory Techn.*, vol. 66, no. 12, pp. 5472–5481, Dec. 2018, doi: 10.1109/TMTT.2018.2860023.
- [14] A. Kord, D. L. Sounas, and A. Alù, "Pseudo-linear time-invariant magnetless circulators based on differential spatiotemporal modulation of resonant junctions," *IEEE Trans. Microw. Theory Techn.*, vol. 66, no. 6, pp. 2731–2745, Jun. 2018, doi: 10.1109/TMTT.2018.2818152.
- [15] X. Wu et al., "Isolating bandpass filters using time-modulated resonators," *IEEE Trans. Microw. Theory Techn.*, vol. 67, no. 6, pp. 2331–2345, Apr. 2019, doi: 10.1109/TMTT.2019.2908868.
- [16] D. Simpson and D. Psychogiou, "Magnet-less non-reciprocal bandpass filters with tunable center frequency," in *Proc. 49th Eur. Microw. Conf. (EuMC)*, Oct. 2019, pp. 460–463, doi: 10.23919/EuMC.2019.8910732.
- [17] D. Simpson and D. Psychogiou, "Fully-reconfigurable non-reciprocal bandpass filters," in *IEEE MTT-S Int. Microw. Symp. Dig.*, Aug. 2020, pp. 807–810, doi: 10.1109/IMS30576.2020.9224096.
- [18] A. Alvarez-Melcon, X. Wu, J. Zang, X. Liu, and J. S. Gomez-Diaz, "Coupling matrix representation of nonreciprocal filters based on timemodulated resonators," *IEEE Trans. Microw. Theory Techn.*, vol. 67, no. 12, pp. 4751–4763, Dec. 2019, doi: 10.1109/TMTT.2019.2945756.
- [19] Z. Yong, Z. Jian, Y. Yuanwei, C. Chen, and J. S. Xing, "A Ku-Band Novel Micromachined Bandpass Filter with Two Transmission Zeros," no. August, 2013.
- [20] G. Chaudhary and Y. Jeong, "Nonreciprocal Bandpass Filter Using Mixed Static and Time-Modulated Resonators," in *IEEE Microwave and Wireless Components Letters*, vol. 32, no. 4, pp. 297-300, April-2022, doi:10.1109/LMWC.2021.3123306.